

UV-curing behavior and physical properties of waterborne UV-curable polycarbonate-based polyurethane dispersion

Hyeon-Deuk Hwang^a, Cho-Hee Park^a, Je-Ik Moon^a, Hyun-Joong Kim^{a,*}, Tetsuo Masubuchi^b

^a Lab. of Adhesion and Bio-Composites, Program in Environmental Materials Science, Seoul National University, Seoul 151-921, Republic of Korea

^b New Coating Business Marketing and Development Department, Performance Coating Materials Division, Asahi Kasei Corporation. Co., Ltd., Jinbocho-Mitsui Bldg., 1-105, Kanda Jinbocho, Chiyoda-ku, Tokyo 101-8101, Japan

ARTICLE INFO

Article history:

Received 8 November 2010

Received in revised form 20 March 2011

Accepted 20 July 2011

Keywords:

UV-curing

Dispersion

Polyurethane

Polycarbonate diol

Photo-DSC

DMA

ABSTRACT

Waterborne UV-curable polyurethane dispersions were synthesized from C5/C6 copolymers of polycarbonate diol(PCDL)s and different end-capping groups. The effects of the polyol molecular weight on the UV-curing behavior and physical properties were examined according to the molecular weight (800, 1000, 2000 g/mol) of PCDL. The UV-curing behavior was analyzed by Fourier transform infrared spectroscopy and photo-differential scanning calorimetry. The influence of the functionality of the end-capping group on the UV-curing behavior and physical properties were also investigated in a similar manner. 2-Hydroxyethylmethacrylate, 2-hydroxyethylacrylate and pentaerythritol tri-acrylate were used to impart mono-methacrylate, mono-acrylate and tri-acrylate functionality to the end-capping group, respectively. The pendulum hardness, curing rate and conversion increased with decreasing molecular weight of the PCDL. The pendulum hardness, curing rate and conversion of dispersion with tri-acrylate functionality on end-capping groups were much higher than those of the other dispersions with mono-methacrylate or mono-acrylate functionality.

© 2011 Elsevier B.V. All rights reserved.

1. Introduction

One of the most important driving forces in the coatings industry and technology is the development of more environmental friendly coatings because consumers are becoming increasingly concerned with environmental issues, and environmental legislation has become more stringent around the world.

Therefore, UV-curing technology has been considered as an alternative to traditional solvent-borne coatings, due to its eco-compatible process and excellent properties, such as high hardness, gloss, scratch and chemical resistance resulting from the high crosslink density from the acrylate group [1,2]. However, UV curable coatings have distinct disadvantages such as volatility, odor, and toxicity because of the low molecular weight monomer used to decrease the viscosity. Waterborne coatings (emulsion or dispersion) are other environmental friendly coatings, that employ water as solvent, and are usually uncrosslinked. Therefore, dry films have drawback such as poor blocking and scratch resistance and low gloss [3,4].

These two technologies have merged into waterborne UV-curable coatings to overcome drawbacks each other and combine

their advantages. The low molecular weight monomers, which are used as reactive diluents to decrease viscosity and the main cause for drawbacks of UV-curing system, are not needed in waterborne UV-curable system. Because UV-curable dispersions are based on high molecular weight binders that make it possible to obtain the low viscosity, it is necessary for spray applications to be independent of the molecular weight of the dispersed polymer. In dispersions, the viscosity is determined by the particle size and concentration. Therefore, the volatility and toxicity, flammability, and odor of the unreacted monomers can be reduced. Moreover, adhesion problems resulting from high volume shrinkage can be avoided because the physical dried films after water evaporation can endure stress and shrinkage and form a tack-free surface, even though they are not crosslinked chemically. The physical or chemical properties of waterborne can be improved by adoption crosslinking structure through UV-curing. Therefore, waterborne UV-curable coatings have a very good hardness-elasticity balance as well as better scratch and chemical resistance than conventional waterborne coatings. On the other hands, this system has some disadvantages. First of all, water has to be driven out of the film by conventional dryers, microwave dryers and/or IR lamps before UV curing. As a result, the longer drying times and higher energy consumption can be required. In addition, application and curing must be carried out under defined climatic conditions, such as proper temperature and low atmospheric humidity [2,5,6].

* Corresponding author. Tel.: +82 2 880 4784; fax: +82 2 873 2318.

E-mail address: hjokim@snu.ac.kr (H.-J. Kim).

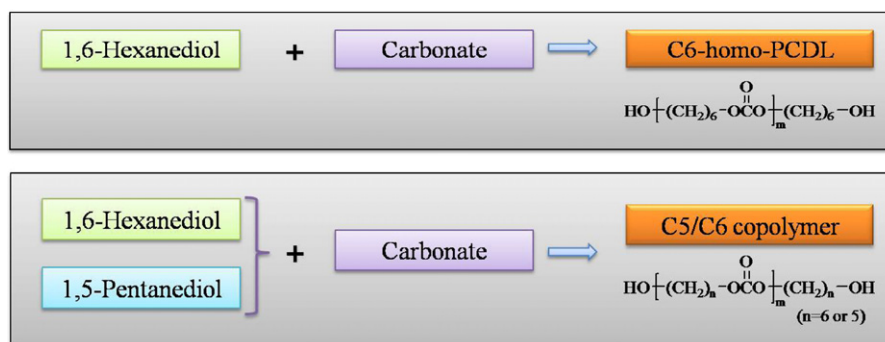


Fig. 1. Comparison of C6 homo polycarbonate diol with C5/C6 copolymer polycarbonate diol.

Waterborne UV-curable systems can be divided into three designs, emulsions, water-soluble resins, or dispersions [5,7]. In the early stage of development, waterborne UV-curable systems were made from unsaturated conventional binders, which were emulsified using polymeric amphiphilic surfactants to form a protective colloid. However, it was very difficult to find the appropriate species and surfactant contents to each system. Another type is a water soluble system, which can dissolve easily into water and can reduce the viscosity using water as a thinner. This type is ideal but water soluble UV-curable resins are rare and their properties are quite poor. The third method is dispersion, which can be made by incorporating dispersing groups, such as hydrophilic or ionic groups, into the backbone of resins. Generally, dispersion exhibits a better hardness-elasticity balance, adhesion strength and chemical resistance, as well as better substrate wetting. In addition, a tack-free film that is already capable of withstanding stress can be acquired only after water drying [3,6].

Of the polyurethanes polyols, polycarbonate polyols are synthesized by two steps, the ester exchange reaction and condensation reaction of monomer diol (e.g. hexanediol) and carbonate monomer (e.g. ethylene carbonate). Aliphatic polycarbonates are used as both binders in high-quality polyurethane coatings and in the production of polyurethane binders, particularly polyurethane dispersion [8,9].

In this study, polycarbonate diol(PCDL)s were used as polyols, to improve physical properties for surface coatings applications because PCDLs have stronger structures than other polyols. The PCDLs used in the synthesis were C5/C6 copolymers, which were prepared from 1,6-hexanediol, 1,5-pentanediol and ethylene carbonate (Asahi Kasei Chemicals Corp.). Fig. 1 shows the differences between C6 homo PCDL and C5/C6 copolymer PCDL. The C5/C6 copolymer has lower viscosity, better weather stability and very good resistance to hydrolysis [10–12].

In this study, polycarbonate-based polyurethane dispersions were synthesized and the effects of molecular weight of polyol and functionality of end-capping groups on the UV-curing behavior and physical and viscoelastic properties were investigated. To examine effects of the chain length of polyol, polyurethane were synthesized with C5/C6 copolymers of polycarbonate with different molecular weights (800, 1000, 2000 g/mol) and isophorone diisocyanate. Dimethylolpropionic acid (carboxyl groups) was incorporated into the polyurethane main chain for self-emulsification. In addition, three types of hydroxyethyl(meth)acrylate (2-hydroxyethylmethacrylate, 2-hydroxyethylacrylate, and pentaerythritol tri-acrylate) were end-capped to determine the effect of the functionality of end-capping groups. The synthesized resins were then neutralized with triethyl amine (base) and dispersed in an aqueous medium with a radical type photo-initiator.

After making the dispersions, UV-curing behavior was investigated using two different methods (Fourier transform infrared

(FT-IR) and photo-differential scanning calorimetry (photo-DSC)), then the conversion and the curing rate were compared. The pendulum hardness and tensile strength were measured to evaluate the physical properties. The viscoelastic properties and glass transition temperatures were measured by dynamic mechanical analysis.

2. Experimental

2.1. Materials

Table 1 shows the chemical structures and properties of raw materials used in this study. Three kinds of polycarbonate diols (PCDL, Asahi Kasei Chemicals Corp.) and dimethylolpropionic acid (DMPA, Across Organics) were dried and degassed at 80 °C under vacuum for 6 h. Isophorone diisocyanate (IPDI, Bayer Material Science) and triethylamine (TEA, Samchun Pure Chemical) were dried using a 4 Å molecular sieve prior to use. One of three hydroxyethyl(meth)acrylate, 2-hydroxyethylmethacrylate (2-HEMA, Junsei Chemicals) or 2-hydroxyethylacrylate (2-HEA, Junsei Chemicals) or pentaerythritol tri-acrylate (PENTA, Sigma Aldrich), was used as an end-capping agent without further purification. The radical type photo-initiator (Irgacure 500, Ciba Specialty Chemicals) was used as received.

2.2. Synthesis of UV-curable polycarbonate-based polyurethane dispersion

Fig. 2 shows the synthesis process of UV-curable polycarbonate-based polyurethane dispersion and Table 2 lists the formulations for the synthesis. A 300 ml round bottom flask equipped with a four-necked separable flask with a mechanical stirrer, thermometer and condenser with drying tube and N₂ inlet were used as the reactor. A constant temperature heating mantle was used to control the reaction temperature at each reaction step. In the first step, IPDI was charged into the dried flask with constant stirring and the temperature was increased to 70 °C. PCDL was dropped for 2 h with some of the catalyst (dibutyltin dilaurate, about 500 ppm) that was maintained for another 1 h. All reactions were monitored and the reaction time at each step was determined by observing the FT-IR peak at 2265 cm⁻¹ (NCO peak). In second step, DMPA as an ionic group was dropped for 1.5 h and reacted for 1 h. In the third step, the reaction temperature cooled to 50 °C, and one of hydroxyethyl(meth)acrylate was dropped for 2 h and reacted for 3 h until the NCO peak had almost disappeared. TEA was then added as a neutralizing agent and stirred for a further 0.5 h after cooling to ambient temperature. In the next step, water was mixed and stirred at 3000 rpm for 1 h. For UV-curing initiation, Irgacure 500 (3 wt%) was added as a photo-initiator.

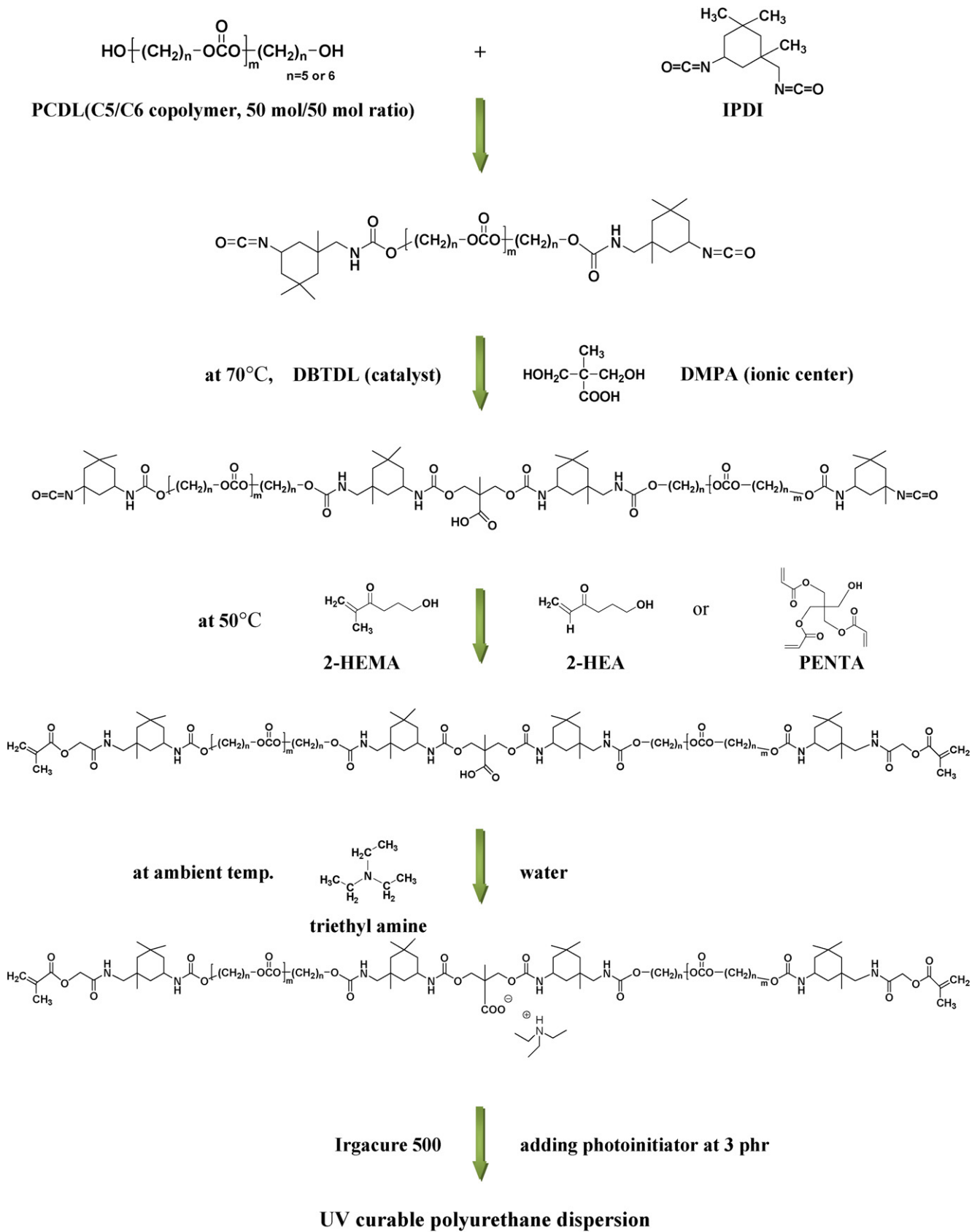
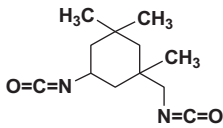
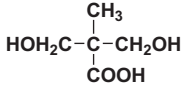
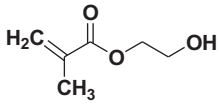
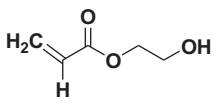
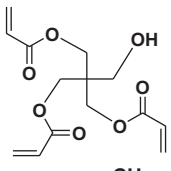
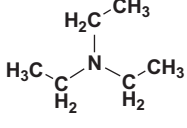
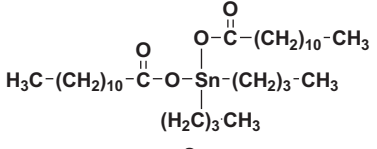
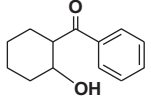
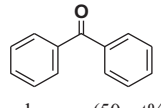


Fig. 2. Synthesis process of the polycarbonate-based UV-curable polyurethane dispersion.

Table 1
Raw materials used for synthesis.

Function	Materials	Chemical structure	Molecular weight (g/mol)	Supplier
Polyol	Polycarbonate diol	$\text{HO}-(\text{CH}_2)_n-\text{O}-\text{CO}-\text{O}-(\text{CH}_2)_m-\text{OH}$ n=5 or 6	800, 1000, 2000	Asahi Kasei Chemicals Corp.
Isocyanate	Isophorone diisocyanate		222	Bayer Material Science
Ionomer	Dimethylolpropionic acid		134	Acros Organics
End-capping agent	2-Hydroxyethylmethacrylate		130	Junsei Chemicals
	2-Hydroxyethylacrylate		116	Junsei Chemicals
	Pentaerythritol triacrylate		298	Sigma Aldrich
Neutralizing agent	Triethylamine		101	Samchun Chemicals
Catalyst	Dibutyltin dilaurate		631.6	Alfa Sesar
Photoinitiator	Irgacure 500	 1-hydroxy-cyclohexyl-phenyl-ketone (50 wt%)	204	Ciba Specialty Chemicals
		 benzophenone (50 wt%)	182	

2.3. Coating and curing process

Waterborne UV-curable coatings were cured through 2 step process, water flash-off and UV-curing step. In water flash-off

step, the physical entanglements occurred during the aqueous dispersion to the tack-free dried film. In the second UV-curing step, radicals formed by activated photoinitiators broke the acrylate double bond resulting in crosslinking structure [2].

Table 2
Formulations used for synthesis (units in mole).

Sample	Molecular weight of polyol (PCDL)			Isocyanate (IPDI)	End-capping group			Ionomer (DMPA)	Neutralizer (TEA)
	800	1000	2000		2-HEMA	2-HEA	PENTA		
WPCU-L800-1MA	0.185			0.444	0.185			0.093	0.093
WPCU-L1000-1MA		0.185		0.444	0.185			0.093	0.093
WPCU-L2000-1MA			0.185	0.444	0.185			0.093	0.093
WPCU-L800-1A	0.185			0.444		0.185		0.093	0.093
WPCU-L800-3A	0.185			0.444			0.185	0.093	0.093

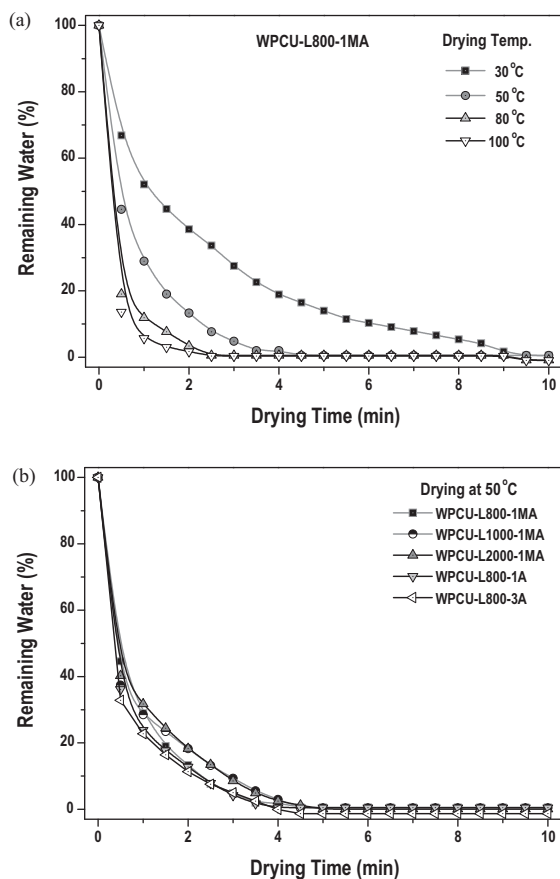


Fig. 3. Water drying rate of WPCU-L800-1MA (a) according to drying temperature and (b) different UV-curable polyurethane dispersions at 50 °C.

Polycarbonate-based polyurethane dispersions were applied onto the glass plate at 40 μm thickness. Water was dried at different temperatures, 30 °C, 50 °C, 80 °C and 100 °C under oven conditions. The remaining water was measured by gravimetry upon water drying time as shown in Fig. 3. The water drying rate was increased with increasing temperatures. The water was dried fast from the beginning and residual water was nearly zero after 5 min at 50 °C. The higher temperature water was dried at, the faster the residual water was decreased. After only 3 min at 80 °C, the residual water was nearly zero. Because of these result, 80 °C and 5 min were selected as the drying temperatures and time, respectively.

The tack-free dried films were then cured by passing under a conveyor type UV-curing machine equipped with medium pressure mercury UV-lamps (100 W/cm, main wave length: 365 nm). The irradiated UV-doses were 250, 500, 1000, 1500, 2000, 2500, and 3000 mJ/cm^2 . The UV doses were measured using an UV radiometer (IL 390C Light Bug, International Light Inc.). To measure the tensile strength and perform dynamic mechanical analysis, the dispersions were casted on an aluminum pan and dried at ambient temperature for 1 day and then, dried in an oven at 60 °C for 1 day. The thickness of fully dried film was 500–600 μm . The dried film was cured using a conveyor type UV-curing machine at UV dose of 3000 mJ/cm^2 .

2.4. Curing behavior and physical and viscoelastic properties

2.4.1. Average particle size

The average particle size of the dispersion was measured at ambient temperature using an electrophoretic light scattering spectrophotometer (ELS-8000, Otsuka Electronics). The dispersion was diluted to about 1% concentration with deionized water, and the measurements were carried out twice.

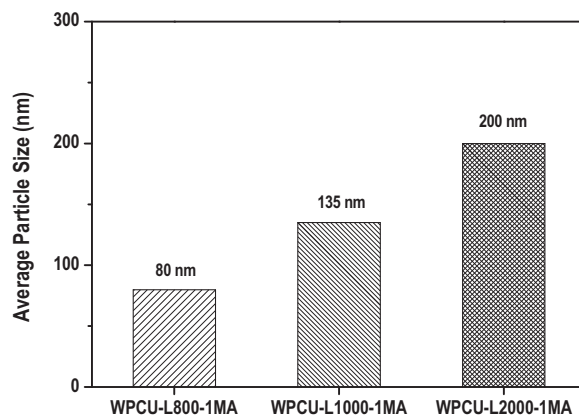


Fig. 4. Average particle size of the dispersion according to the different molecular weights of polycarbonate diol.

2.4.2. Monitoring synthesis process and UV-curing behavior by Fourier transform Infrared (FT-IR) spectroscopy

The FT-IR spectra were used for two purposes, monitor the polyurethane reaction and evaluate the UV-curing behavior. Polyurethane synthesis was controlled by monitoring the disappearance of the characteristic peaks of the NCO groups (2265 cm^{-1}). The UV-curing behavior was evaluated by observing the changes in the deformation of the C=C bond at 1635 or 810 cm^{-1} . Acrylate double bond conversion after a given irradiation time (t) was calculated using following equation:

$$\text{Conversion}(\%) = \frac{(A_{810})_0 - (A_{810})_t}{(A_{810})_0} \times 100 \quad (1)$$

where $(A_{810})_0$ is the intensity of 810 cm^{-1} at initial time and $(A_{810})_t$ is the intensity of 810 cm^{-1} at time t . The IR spectra were recorded on a JASCO FT/IR-6100 (Japan) equipped with a Miracle accessory, which is a type of attenuated total reflectance made from ZnSe. The FT-IR spectra were recorded from 4000 to 650 cm^{-1} and at 4 cm^{-1} resolution.

2.4.3. UV-curing behavior by photo differential scanning calorimetry (photo-DSC)

To examine the UV-curing behavior, the photo-DSC experiments were carried out using a DSC (Q-1000, TA Instruments) equipped with a photocalorimetric accessory (Novacure 2100), which employed light from a 100 W medium-pressure mercury

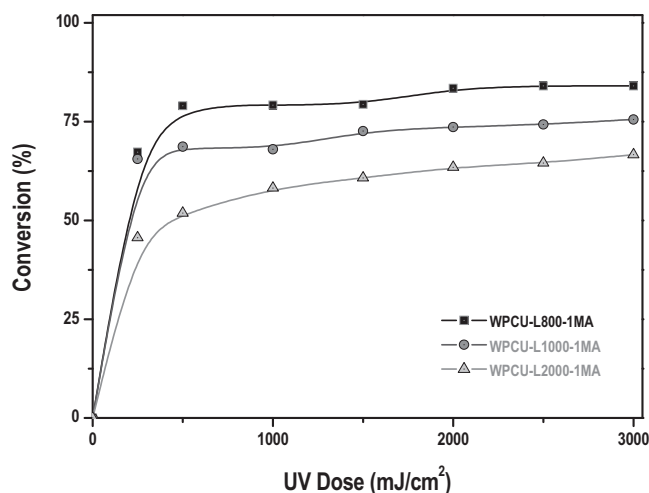


Fig. 5. C=C double bond conversion with increasing UV-dose according to the different molecular weights of the polycarbonate diol by FT-IR.

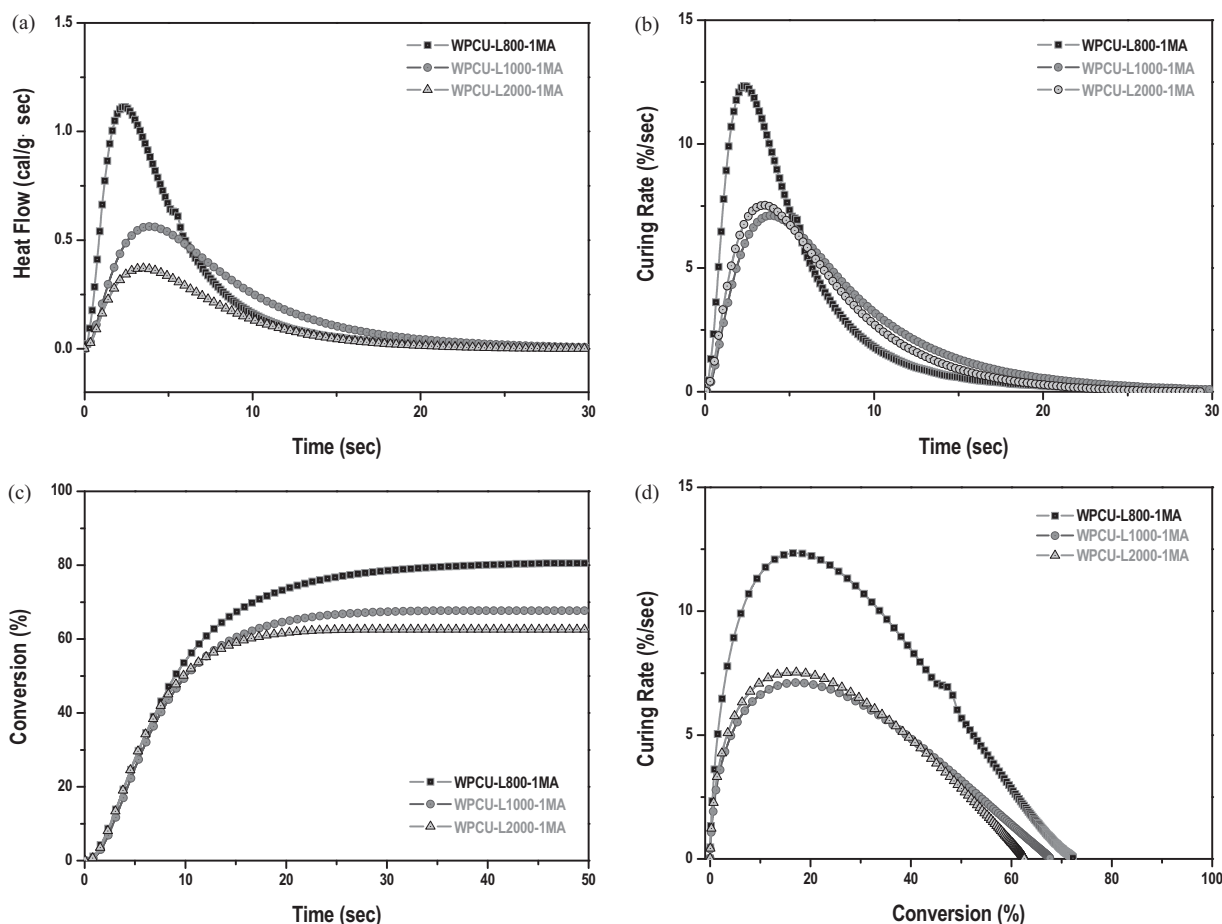


Fig. 6. Isothermal UV-curing heat enthalpy and conversion profiles for polyurethane dispersions synthesized using polycarbonate diol with different molecular weights by photo-DSC. (a) Heat flow vs. time, (b) conversion vs. time, (c) curing rate vs. time, and (d) curing rate vs. conversion.

lamp (main wave length: 250–650 nm). The light intensity was determined by placing an empty DSC pan on the sample cell. The UV light intensity at the sample was 50 mW/cm². The weight of the sample was approximately 2 mg and the sample was placed in an open aluminum DSC pan. Before UV curing, the water contained in samples was evaporated at 50 °C for 10 min. The measurements were carried out at 30 °C in flowing N₂ gas at 50 ml/min.

2.4.4. Viscoelastic properties by dynamic mechanical analysis (DMA)

The viscoelastic properties of cured films were measured using a DMA instrument (Q800, TA Instruments). Rectangular specimens, 12 mm in length, 6.6 mm in width and 0.5 mm in thickness were prepared. The measurements were taken in tension mode at a frequency of 1 Hz and strain of 0.1%. The temperature ranged from –100 °C to 150 °C at scanning rate of 2 °C/min. The storage modulus (E'), loss modulus (E'') and loss factor ($\tan \delta$) of the cured films were measured as a function of temperature.

2.4.5. Pendulum hardness

The change in surface hardness at different UV dose was determined by measuring the pendulum hardness at 23 ± 2 °C and 50 ± 3% R.H. using a pendulum hardness tester (Ref. 707PK, Sheen Instruments Ltd.) according to the König method (ASTM D 4366).

2.4.6. Tensile strength

The tensile strength was measured using a Universal Testing Machine (Zwick Corp.) at ambient temperature with a crosshead

speed of 100 mm/min. Rectangular specimens, 20 mm in length (span length), 6.6 mm in width and 0.5 mm in thickness, were prepared. Five measurements were conducted and the mean value was used.

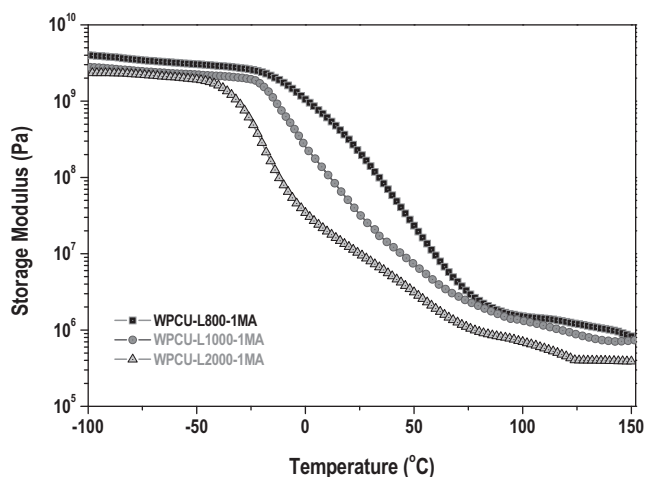
3. Results and discussion

3.1. Effect of molecular weight of polycarbonate diol

3.1.1. Average particle size of the dispersions

Several factors affect the particle size of the dispersion. The hydrophobicity, which is determined by the ionic group content and prepolymer molecular weight, has a significant effect on the particle size of dispersion. The main chain flexibility and molecular structure also influence the particle size. In the case of a flexible structure with ionic groups chain in soft segment, finer particles can be found in the dispersion because the tailoring of ionic groups to the surface during the dispersion process takes place easily due to the easier conformation change in the soft segment [13,14]. In particular, the particle of dispersion depends strongly on the viscosity of the dispersant and ionic group content.

Fig. 4 shows the average particle size of the dispersions according to the different molecular weight of the PCDL. The average particle size of the dispersions increased with increasing molecular weight of the PCDL. The average particle size of WPCU-L2000-1MA was 200 nm, which was as 2.5 and 1.5 times higher than that of WPCU-L800-1MA (80 nm) and WPCU-L1000-1MA (135 nm), respectively, because higher molecular weight of polyol gives higher viscosity and lower ionomer content (by weight). An almost



(a) Storage modulus

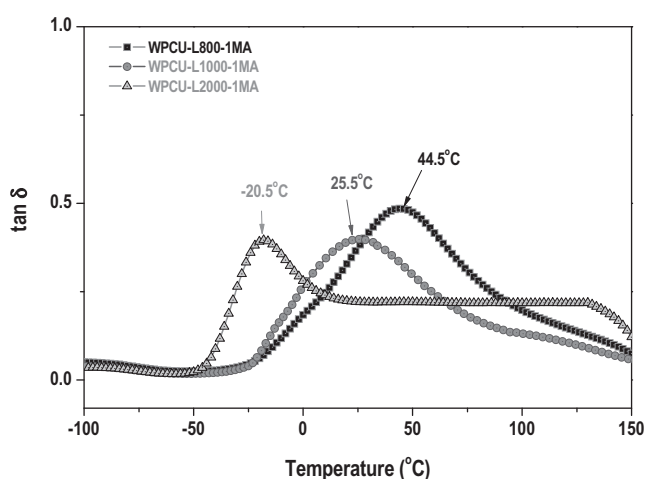
(b) $\tan \delta$

Fig. 7. Viscoelastic properties of the cured films according to the different molecular weights of polycarbonate diol.

linear correlation was observed between the molecular weight and the average particle size.

3.1.2. C=C double bond conversion by FT-IR spectroscopy

The properties of UV cross-linked films depend strongly on the final C=C double bond conversion achieved after UV irradiation. The strength of the cross-linking structure increased with increasing conversion. The UV-curing behavior was monitored by FT-IR. Fig. 5 shows the conversion curves as a function of the irradiated UV-dose for the three kinds of dispersions synthesized using polyols with different molecular weights. The slope of the conversion curve at the initial curing process means the UV-curing rate and the plateau value at the end of curing indicates the final conversion [15–17].

The C=C double bond conversions of WPCU-L800-1MA and WPCU-L1000-1MA reached a plateau at approximately 84% and 75%, respectively, after only 500 mJ/cm² of UV-irradiation. By comparison, WPCU-L2000-1MA leveled off at approximately 66% after 1500 mJ/cm². The curing rate was faster and the final conversion of WPCU-L800-1MA was higher than that of WPCU-L1000-1MA or WPCU-L2000-1MA, because the dispersion synthesized with the low molecular weight polyol had a higher density of methacrylate double bonds.

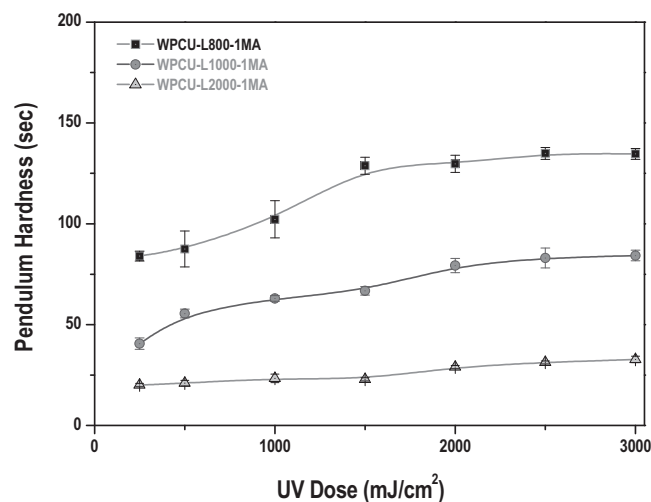


Fig. 8. Pendulum hardness of the cured film as function of the UV-dose for polyurethane dispersions synthesized using polycarbonate diol with different molecular weights.

3.1.3. UV-curing kinetics by photo-DSC

Monitoring UV-curing behavior is not easy because of its extremely rapid curing speed. Photo-DSC and real-time FT-IR measurements are convenient methods for evaluating the reactivity and measuring the kinetics of an in situ UV-curing reaction, which are essential factors for UV-curing applications. The reaction heat released during the UV-curing process depends on the functionality and species of the reacting groups. Fig. 6 shows the isothermal UV-curing heat enthalpy and conversion profiles for polyurethane dispersion synthesized using PCDLs with different molecular weight. In the photo-DSC measurement, heat flow (cal/g s) plotted in Fig. 6(a) is the only result of the measurement and the others (Fig. 6(b)–(d)) are the results of further calculations.

The reaction enthalpy or the conversion of C=C double bonds were calculated by integrating the area under the exothermic peak using the following equation [18,19]:

$$\alpha = \frac{\Delta H_t}{\Delta H_0^{\text{theor}}} \quad (2)$$

where ΔH_t is the reaction heat enthalpy released at time t and $\Delta H_0^{\text{theor}}$ is the theoretical heat enthalpy for the complete conversion. For these calculations, $\Delta H_0^{\text{theor}}$ (acrylate) = 86 kJ/mol (20.6 kcal/mol), and $\Delta H_0^{\text{theor}}$ (methacrylate) = 54.4 kJ/mol (13.1 kcal/mol) [20,21]. And the heat of polymerization of each sample ($\Delta H_0^{\text{theor}}$ (sample)) was calculated using Eq. (3):

$$\Delta H_0^{\text{theor}}(\text{sample}) = \frac{\Delta H_0^{\text{theor}}(\text{acrylate}) / \Delta H_0^{\text{theor}}(\text{methacrylate})}{\text{MW}^{\text{theor}} \times \text{Functionality}} \quad (3)$$

where MW^{theor} is the theoretical molecular weight of the repeating unit. Table 3 lists the calculated values of all samples. For example, MW^{theor} of WPCU-L800-1MA is 2884 (g/mol) and its functionality is 2-methacrylate (26.2 kcal/mol). Therefore, $\Delta H_0^{\text{theor}}$ was calculated to be 9.0 cal/g. This value was placed into the denominator of Eq. (2), and the conversion of all samples was calculated, as shown in Fig. 6(b). The rate of polymerization (R_p) is related directly to the heat flow (dH/dt) using the following equation [18,19]:

$$R_p = \frac{d\alpha}{dt} = \frac{(dH/dt)}{\Delta H_0^{\text{theor}}} \quad (4)$$

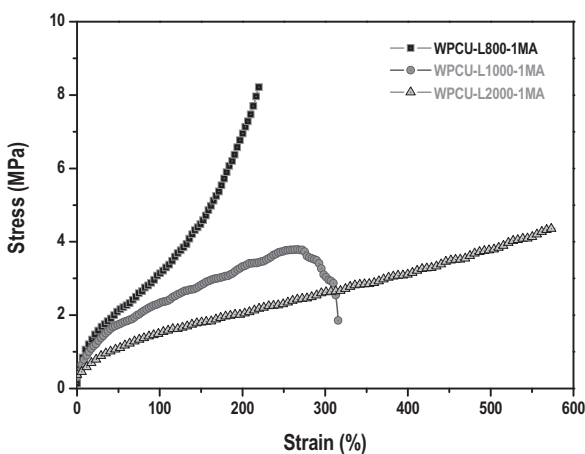
where $d\alpha/dt$ is the conversion rate or the polymerization rate, $\Delta H_0^{\text{theor}}$ is the total exothermic heat of reaction and dH/dt is the

Table 3
Calculated theoretical reaction enthalpy.

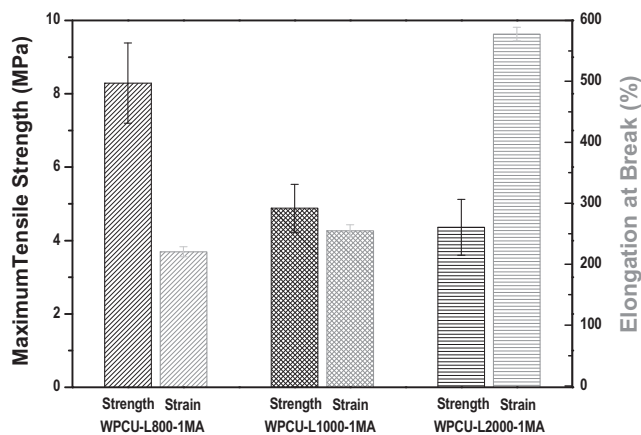
Samples	Theoretical molecular weight of repeating unit	Functionality	Theoretical reaction enthalpy			
			kJ/mol	J/g	kcal/mol	cal/g
WPCU-L800-1MA	2884	2-Methacrylate	108.8	37.7	26.2	9.0
WPCU-L1000-1MA	3284	2-Methacrylate	108.8	33.1	26.2	7.9
WPCU-L2000-1MA	5284	2-Methacrylate	108.8	20.6	26.2	4.9
WPCU-L800-1A	2856	2-Acrylate	172	60.2	41.1	14.4
WPCU-L800-3A	3220	6-Acrylate	516.0	160.3	123.6	38.3

measured heat flow at a constant temperature. Fig. 6(c) shows the result of Eq. (4) and Fig. 6(d) gives a plot of the curing rate (R_p) as a function of the conversion (α).

In Fig. 6(a), the early onset of auto-acceleration by the activation of radicals was confirmed as a steep increase at the beginning of the reaction, which was followed by auto deceleration, as indicated in the rapid dropping curves. The final conversion of WPCU-L800-1MA, WPCU-L1000-1MA and WPCU-L2000-1MA was 72.0%, 67.7% and 62.6%, respectively as shown in Fig. 6(b). The polyurethane dispersion synthesized with shorter chain polyols showed higher final conversion, owing to its higher C=C double bond density. The trends of these results are similar to results of the C=C double bond conversion determined by FT-IR. Fig. 6(c) and Table 4 show the curing rate as function of time and the



(a) Strain-stress curve



(b) Maximum tensile strength and elongation at break

Fig. 9. Tensile behavior of the cured film according to the different molecular weights of polycarbonate diol.

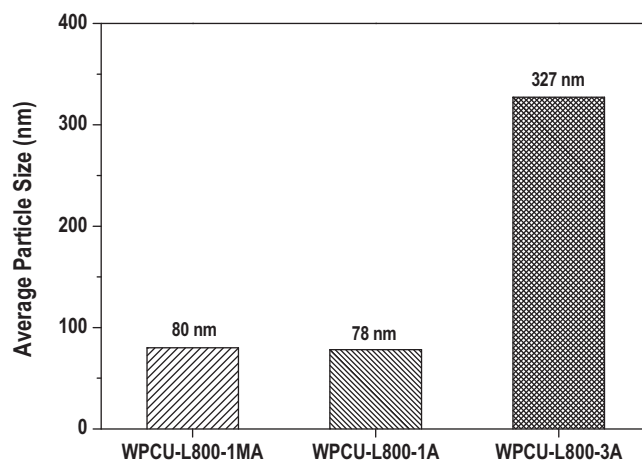


Fig. 10. Average particle size of dispersion according to the functionality of the end-capping group.

peak time with the maximum curing rate. Fig. 6(d) shows a plot of the curing rate versus conversion. The curing rate peak of WPCU-L800-1MA appeared first at 2.35 s, and the maximum curing rate was 12.3%/s, which was higher than other samples. Therefore, the curing rate and conversion increased with decreasing molecular weight of the PCDL incorporated into the backbone, because dispersion synthesized with shorter chain polyol had a higher C=C double bond density and cured faster with higher final conversion.

3.1.4. Viscoelastic properties

Fig. 7 presents the viscoelastic properties of the cured film according to the molecular weight of the PCDL. The viscoelastic

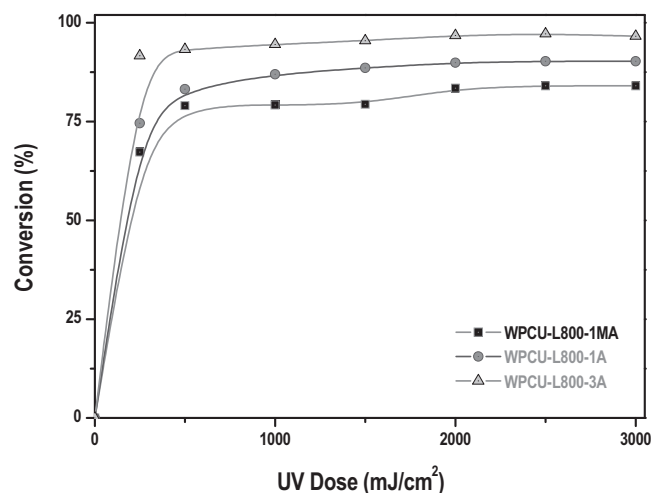


Fig. 11. C=C double bond conversion with increasing UV-dose according to different functionality of the end-capping group by FT-IR.

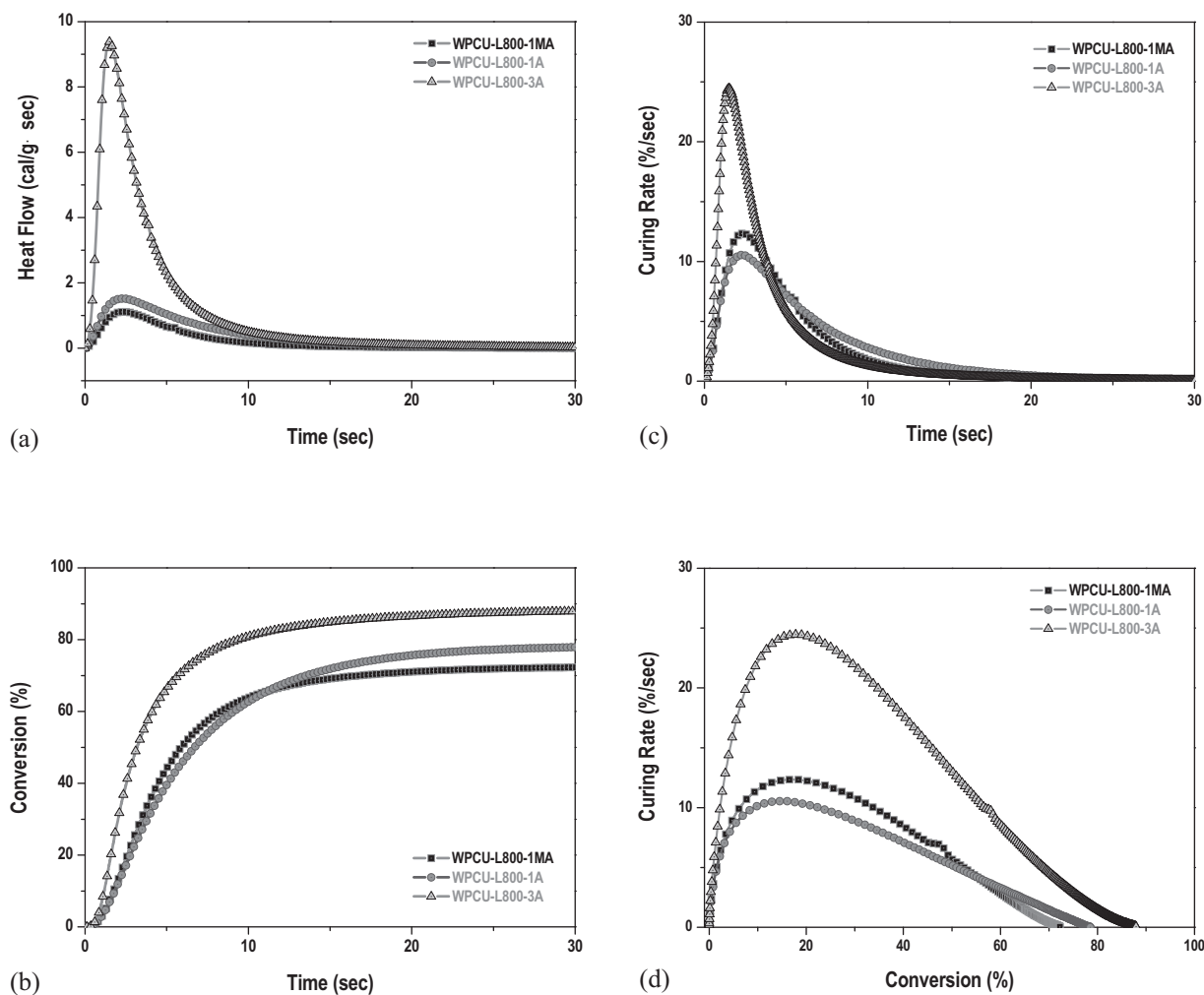


Fig. 12. Isothermal photo polymerization and conversion profiles of polyurethane dispersions synthesized with different functionality of the end-capping group by photo-DSC. (a) Heat flow vs. time, (b) conversion vs. time, (c) curing rate vs. time, and (d) curing rate vs. conversion.

properties are based on the dependence between the degree of cross-linking and the glass transition temperature of the cured samples. As shown in Fig. 7(a), the storage modulus (E') decreased rapidly near the glass transition temperature (T_g) due to vibration of the molecular segments. The decreasing in the storage modulus continued until its rubbery plateau, and the chemical crosslinks were restricted further proceeding to the flowing region. Fig. 7(b) shows the $\tan \delta$ curves of the samples synthesized using the polyols with different molecular weights. The T_g of WPCU-L800-1MA, WPCU-L1000-1MA and WPCU-L2000-1MA was 44.5 °C, 25.5 °C and -20.5 °C, respectively. The change in T_g between WPCU-L1000-1MA and WPCU-L2000-1MA and between WPCU-L800-1MA and WPCU-L1000-1MA was approximately 19 °C, and 46 °C, respectively. As the segmental chain length decreased, the motion of segments was restricted, and the glass transition temperature increased as

a result. In addition, the samples had a single T_g , which meant good miscibility between the hard and soft segments [22].

The crosslink density, which is closely related to the other physical properties, is expressed as ν (mol/g; $0 \leq \nu$) or as the degree of crosslinking (X_c ; $0 \leq X_c \leq 1$). The molecular weight between crosslinks (M_c) is a reciprocal of X_c , which can be calculated using following equation [5]:

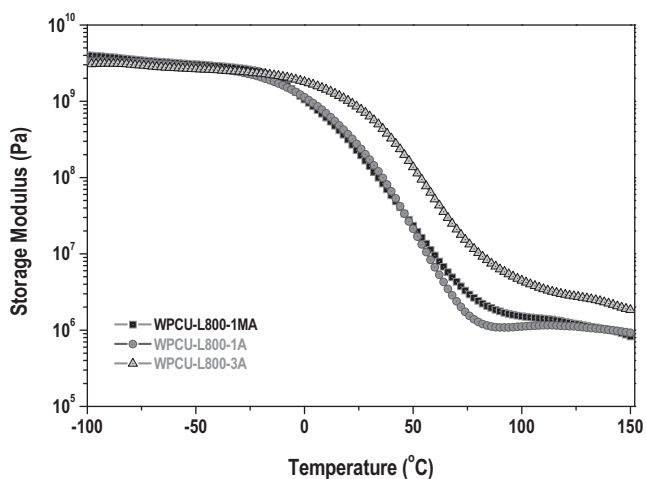
$$M_c = \frac{M}{f - 2} \quad (5)$$

where f is the functionality of the molecule, f value of one double bond is 2. For example, f value of WPCU-L800-1MA or WPCU-L800-1A is same as 4, because they have two double bonds on both chain ends. In the denominator, $f - 2$ is used because a functionality of 2 contributes only to linear molecular weight build-up, but not to branching or crosslinking. In the case where several components

Table 4

Peak time of the curing rate, maximum curing rate, and final conversion by photo-DSC.

Samples	Peak time of curing rate (s)	Maximum curing rate (%/s)	Final conversion (%)
WPCU-L800-1MA	2.35	12.3	72.3
WPCU-L1000-1MA	3.85	7.1	67.7
WPCU-L2000-1MA	3.50	7.5	62.6
WPCU-L800-1A	2.30	10.5	78.5
WPCU-L800-3A	1.50	24.5	88.1



(a) Storage modulus

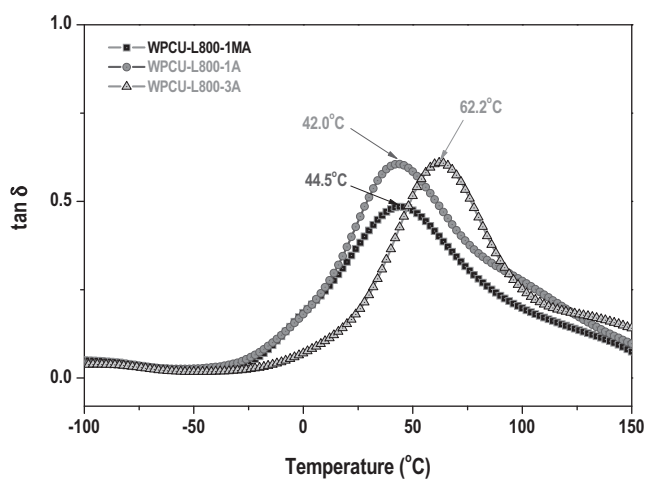
(b) tan δ

Fig. 13. Viscoelastic properties of the cured film according to different functionality of the end-capping group.

are used, the average molecular weight (M_0) and functionality (f_0) are calculated using the following equation:

$$M_0 = \frac{n_1M_1 + n_2M_2 + \dots + n_iM_i}{n_1 + n_2 + \dots + n_i} \quad (6)$$

$$f_0 = \frac{n_1f_1 + n_2f_2 + \dots + n_if_i}{n_1 + n_2 + \dots + n_i} \quad (7)$$

Resulting in

$$M_c = \frac{M_0}{f_0 - 2} \quad (8)$$

The conversion of the functional groups can be determined using the following equation:

$$M_c = \frac{M_0}{pf_0 - 2} \quad (9)$$

where p is the fraction of converted groups ($p \leq 1$) [5]. These calculated results are listed in Table 5. Both the final conversions by FT-IR and photo-DSC measurements were used as p to calculate M_c and X_c . The crosslink density calculated by FT-IR was somewhat higher because the final conversion by FT-IR was higher than that determined by photo-DSC. The crosslink density also can be determined experimentally by dynamic mechanical analysis based

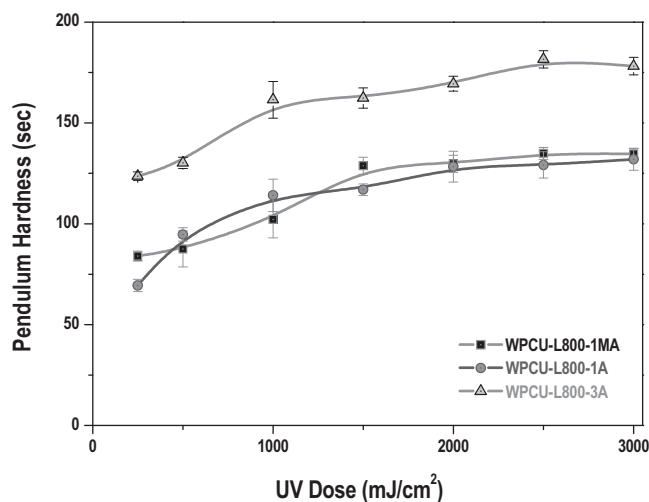


Fig. 14. Pendulum hardness as function of the UV-dose for polyurethane dispersions with different functionality of the end-capping group.

on the theory of rubber elasticity using the following equation [14,23]:

$$G_N^0 = \frac{\rho RT}{M_c} \quad (10)$$

where G_N^0 is the rubbery plateau modulus, ρ is the density, T is the absolute temperature, and R is the gas constant.

Table 5 lists the actual M_c and X_c calculated using Eq. (10). There were some differences compared to the theoretical M_c and X_c calculated using the final conversion by FT-IR and photo-DSC. However, the trends were the same and X_c was in order of WPCU-L2000-1MA < WPCU-L1000-1MA < WPCU-L800-1MA. The crosslink density of the polyurethane dispersion with the shorter chain was higher. In the case of the distance between reacting groups at each end was shorter, the network formed as a denser web during UV-curing process. The crosslink density can be used as a factor to determine the difference in the physical properties of each cured film. A higher crosslink density leads to better physical performance.

3.1.5. Pendulum hardness

Fig. 8 shows the effect of the molecular weight of the polyol on the surface hardness with increasing UV-dose. The pendulum hardness of all samples increased with increasing UV-dose, because the polymer network formed by UV-curing improved the surface hardness. The pendulum hardness of WPCU-L800-1MA (33 s) was higher than that of WPCU-L1000-1MA (84 s) and WPCU-L2000-1MA (132 s) after a UV-dose of 3000 mJ/cm². Regarding WPCU-L800-1MA, the difference in molecular weight between crosslinks (M_c) was lowest and the crosslink density was highest because it was synthesized with the shortest PCDL. The mechanical properties of the systems showed a clear trend in that the flexibility decreases with decreasing molecular weight between crosslinks [5].

3.1.6. Tensile strength

Fig. 9 shows the effect of the molecular weight of polyol on the stress-strain behaviors (a) and the maximum tensile strength and elongation at break (b). The maximum tensile strength and initial modulus (slope of the curve) increased and the elongation at break decreased with decreasing molecular weight of polyol. The network with a high crosslink density had better resistance to an external extension force, which leads to a higher tensile strength and lower elongation at break.

Table 5

Calculated theoretical molecular weight between the crosslinks (M_c) and degree of crosslinking (X_c) using final conversion measured by FT-IR and photo-DSC, actual M_c and X_c measured by DMA.

Samples	Theoretical molecular weight	Functionality	Theoretical M_c and X_c by FT-IR			Theoretical M_c and X_c by photo-DSC			Actual M_c and X_c by DMA	
			Final conversion (%)	M_c (g/mol)	$X_c (\times 10^3)$	Final conversion (%)	M_c (g/mol)	$X_c (\times 10^3)$	M_c (g/mol)	$X_c (\times 10^3)$
WPCU-L800-1MA	2884	4 (2 double bond)	84.2	2108	0.474	72.3	3277	0.305	2708	0.369
WPCU-L1000-1MA	3284	4 (2 double bond)	75.6	3207	0.312	67.7	4638	0.216	4289	0.233
WPCU-L2000-1MA	5284	4 (2 double bond)	66.6	7958	0.126	62.6	10,484	0.095	7856	0.127
WPCU-L800-1A	2856	4 (2 double bond)	90.2	1776	0.563	78.5	2505	0.399	2783	0.359
WPCU-L800-3A	3220	12 (6 double bond)	96.5	336	2.975	88.1	376	2.662	784	1.276

3.2. Effect of functionality of end-capping group

3.2.1. Average particle size of dispersion

Fig. 10 shows the relationship between the average particle size and the functionality of the end-capping groups. The average particle size of WPCU-L800-1MA (80 nm) and WPCU-L800-1A (78 nm) were similar. However, the average particle size of WPCU-L800-3A (325 nm) was much larger than those of the other dispersions. As mentioned above, the hydrophobicity of the dispersion affects the particle size. WPCU-L800-3A had bulky tri-acrylate groups on each end of the chain, which increased the hydrophobicity. As a result,

the average particle size of WPCU-L800-3A was much larger than the other dispersions with smaller mono-methacrylate or mono-acrylate groups on the each end of the chain.

3.2.2. C=C double bond conversion by FT-IR spectroscopy

Fig. 11 shows the effect of the functionality of the end-capping groups on the C=C double bond conversion during the UV-curing process by FT-IR. The curing rate and final conversion depended strongly on the functionality of the dispersion. The conversion of WPCU-L800-3A was above 90% only after UV-dose of 250 mJ/cm² and the final conversion reached 96.5%. On the other hands, the final conversion for WPCU-L800-1MA and WPCU-L800-1A was 84.2% and 90.2%, respectively. The curing speed of the tri-functionality was much faster than that of the mono-methacrylate or mono-acrylate functionality. In addition, more complete curing was achieved by increasing the functionality.

3.2.3. UV-curing kinetics by photo-DSC

The rate of UV-curing depends on several factors, the intensity of UV-light, photo-initiator concentration and the reactivity of functional groups as well as their concentration [18]. Fig. 12 shows the effect of the functionality of the end-capping groups on the UV-curing behavior by photo-DSC measurement. Using the same method in Fig. 6, the conversion and curing rate were calculated and plotted in Fig. 12(b)–(d). The curing rate and conversion of WPCU-L800-3A with tri-acrylate functionality were much higher than those of the other samples with mono-methacrylate or mono-acrylate functionality. The final conversion was in the following order: WPCU-L800-1MA (72.0%) < WPCU-L800-1A (80.5%) < WPCU-L800-3A (88.3%). Fig. 14(c) and Table 4 show the curing rate as function of time and the peak time with the maximum curing rate. The curing rate peak of WPCU-L800-3A appeared first at 1.50 s and the maximum curing rate was 24.5%/s, which was much higher than the other samples. Therefore, the curing rate and conversion increased with increasing the functionality of the end-capping groups, because coatings with higher functionality are easily activated and continued the reaction.

3.2.4. Viscoelastic properties

Fig. 13 shows the relationship between the functionality of the end-capping groups and the viscoelastic properties. The T_g of WPCU-L800-1MA and WPCU-L800-1A were similar, 44.5 °C and 42.0 °C, respectively. However, the T_g of WPCU-L800-3A was higher (62.2 °C) owing to its higher functionality, which produced a network structure with a higher crosslink density. This can be confirmed by the theoretical and actual M_c and X_c . There were some differences between methods, but the order of the crosslink density was as following: WPCU-L800-1MA \leq WPCU-L800-1A < WPCU-L800-3A. In particular, the theoretical X_c of WPCU-L800-1A was higher than that of WPCU-L800-1MA but the actual X_c of both was similar. Even though the activity of methacrylate is lower than acrylate, the physical properties of polymer with

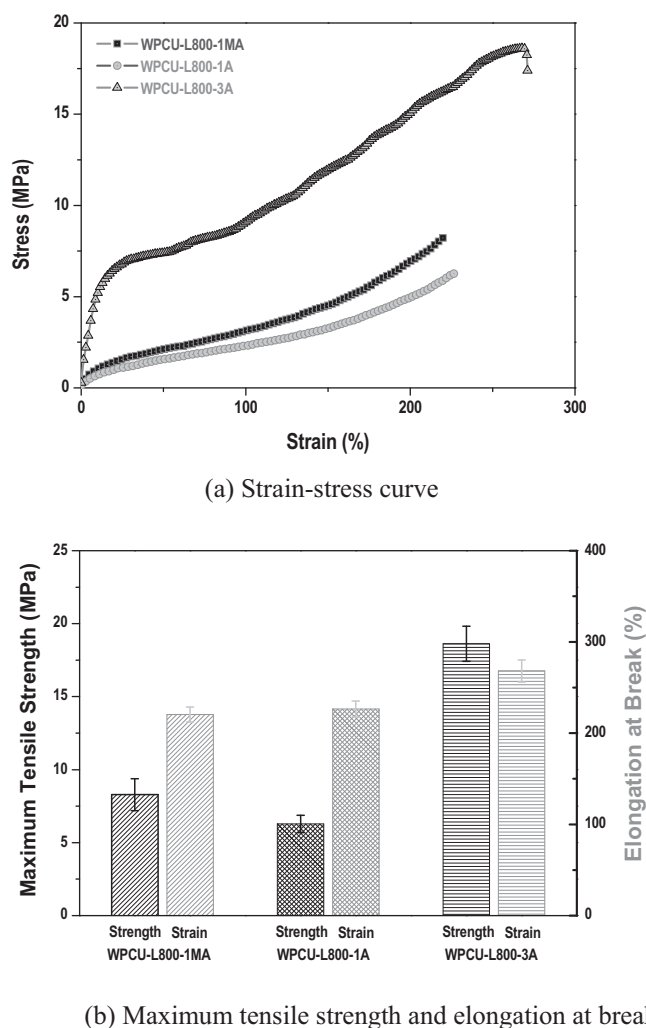


Fig. 15. Tensile behavior of the cured film according to different functionality of the end-capping group.

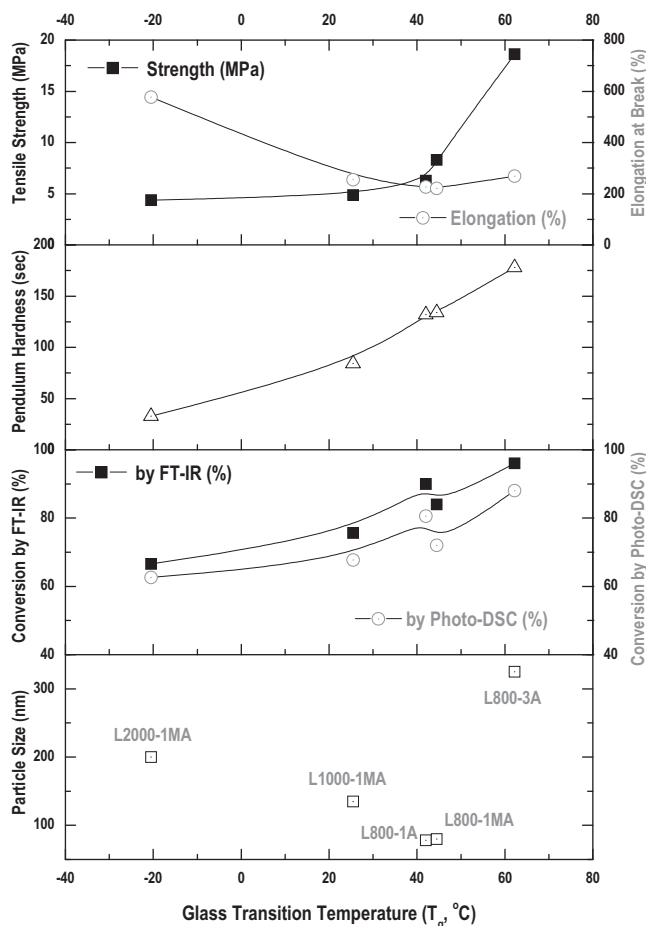


Fig. 16. Correlation between the glass transition temperature and the other properties.

methacrylate are better with acrylate due to its molecular structure (e.g. T_g of polymethylmethacrylate (105 °C) > polymethylacrylate (9 °C)). The crosslink density and T_g increased with increasing the functionality and the physical properties also improved.

3.2.5. Pendulum hardness

Fig. 14 shows the effect of functionality on the surface hardness as function of UV-dose. The pendulum hardness of WPCU-L800-3A with tri-acrylate functionality in end-capping groups was higher than that of WPCU-L800-1MA and WPCU-L800-1A, which had mono-methacrylate or mono-acrylate functionality. The network structure of the cured coatings with mono-functionality was formed as a low crosslink density and tri-functionality produced a higher crosslinkable network structure. Generally, a high crosslinking density is responsible for the high hardness. The weak physical properties of waterborne system can be improved by incorporating multi-functional end-capping groups.

3.2.6. Tensile strength

Fig. 15 presents the relationship between the functionality and tensile behaviors. There were many differences in the initial modulus and maximum tensile strength between WPCU-L800-1MA and WPCU-L800-1A. In addition, the elongations at break were similar due to their comparable functionality. Generally, there is a trade-off between the strain properties and tensile strength. However, WPCU-L800-3A showed a very high initial modulus and maximum tensile strength as well as a very high elongation at break.

The elongations at break of all samples were over than 100%. The restricted application area of UV-curable coatings due to their very

low extensibility can be expanded to certain coating applications that require high extensibility, such as coatings for pre-primed or pre-coated metal sheet. In these applications, the coating layers are coated in-line during manufacturing metal sheet process, which then follows the forming process, such as deep drawing. Therefore, the high extensibility and high maximum tensile strength are essential properties to obtain the balance between formability and physical properties in pre-coated metal sheet application [24,25].

3.3. Correlation between glass transition temperature with other properties

Among the properties measured in this study, the glass transition temperature showed a very interesting correlation with the other properties. As mentioned above, the T_g increased with decreasing molecular weight of the polyol or increasing functionality of the end-capping groups. Fig. 16 shows the correlation between the T_g with final conversion, pendulum hardness, maximum tensile strength and elongation at break. There was no correlation between the T_g and average particle size because the average particle size is governed by the molecular weight of polyol or the hydrophobicity resulting from the molecular structures. Both of the final conversion curves by FT-IR and photo-DSC increased consistently with increasing T_g because higher conversion produced more intensive networks and led to a higher T_g of cured film. The pendulum hardness showed a linear correlation with T_g because both are physical properties formed by other factors. The maximum tensile strength also increased with increasing T_g . In particular, the strength increased considerably with increasing of the functionality (WPCU-L800-1MA → WPCU-L800-3A). By contrast, the elongation at break decreased with increasing T_g . A steep decline was observed between WPCU-L2000-1MA and WPCU-L1000-1MA, which means that the chain length between networks has a greater effect on the strain properties than the functionality.

4. Conclusions

C5/C6 copolymers of PCDLs were used to synthesize waterborne UV-curable polyurethane dispersions. The effect of polyol molecular weight and functionality on the curing behavior and physical properties were examined using PCDLs with different molecular weights and end-capping groups with different functionality. The curing rate and final conversion increased with decreasing molecular weight of the polyol, and the physical properties, such as pendulum hardness and maximum tensile strength, increased because dispersions synthesized with shorter chain polyol have higher reactivity and form more intensive polymer networks. The pendulum hardness, curing rate and final conversion of WPCU-L800-3A with tri-acrylate functionality were much higher than those of the other dispersions with mono-methacrylate or acrylate functionality. Therefore, the physical properties of the waterborne UV-curable coatings were improved by incorporating PCDL with a low molecular weight and multifunctional end-capping groups. The glass transition temperature of cured films showed a good correlation with the other physical properties.

Acknowledgements

This study was supported partially by Industrial Strategic Technology Development Program (10035163) – “Development of highly flexible pre-finished color metal sheet and modular process technology for automotive”, Ministry of Knowledge and Economy, Republic of Korea.

References

- [1] M. Nanea, High Solid Binders, Vincentz Network, Hannover, 2008.
- [2] H.-D. Hwang, J.-I. Moon, J.-H. Choi, H.-J. Kim, S.D. Kim, J.C. Park, Effect of water drying conditions on the surface property and morphology of waterborne UV-curable coatings for engineered flooring, *J. Ind. Eng. Chem.* 15 (2009) 381–387.
- [3] J.S.J. Pruskowski, Waterborne Coatings Technology, Federation of Societies for Coatings Technology, Blue Bell, PA, 2004.
- [4] J.Z.W. Wicks, F.N. Jones, S.P. Pappas, D.A. Wicks, Organic Coatings: Science and Technology, 3rd ed., John Wiley & Sons, Inc., Honoke, New Jersey, 2007.
- [5] R. Schwalm, UV Coatings: Basics, Recent Developments and New Applications, Elsevier, Amsterdam, London, 2007.
- [6] P. Glöckner, T. Jung, S. Struck, K. Studer, Radiation Curing—Coatings and Printing Inks, Vincentz Network, Hannover, 2008.
- [7] R. Schwalm, L. Haussling, W. Reich, E. Beck, P. Enenkel, K. Menzel, Tuning the mechanical properties of UV coatings towards hard and flexible systems, *Prog. Org. Coat.* 32 (1997) 191–196.
- [8] U. Meier-Westhues, Polyurethanes: Coatings, Adhesives and Sealants, Vincentz Network, Hannover, 2007.
- [9] S. Nakano, Polycarbonate-modified acrylic polymers for coating materials, *Prog. Org. Coat.* 35 (1999) 141–151.
- [10] T. Masubuchi, H. Fukumura, H. Masuhara, K. Suzuki, N. Hayashi, Laser-induced decomposition and ablation dynamics studied by nanosecond interferometry—3. A polyurethane film, *J. Photochem. Photobiol. A* 145 (2001) 215–222.
- [11] M. Furukawa, Y. Hamada, K. Kojio, Aggregation structure and mechanical properties of functionally graded polyurethane elastomers, *J. Polym. Sci. Polym. Phys.* 41 (2003) 2355–2364.
- [12] K. Kojio, Y. Nonaka, T. Masubuchi, M. Furukawa, Effect of the composition ratio of copolymerized poly(carbonate) glycol on the microphase-separated structures and mechanical properties of polyurethane elastomers, *J. Polym. Sci. Polym. Phys.* 42 (2004) 4448–4458.
- [13] B.K. Kim, J.S. Yang, S.M. Yoo, J.S. Lee, Waterborne polyurethanes containing ionic groups in soft segments, *Colloid Polym. Sci.* 281 (2003) 461–468.
- [14] B.K. Kim, B.U. Ahn, M.H. Lee, S.K. Lee, Design and properties of UV cured polyurethane dispersions, *Prog. Org. Coat.* 55 (2006) 194–200.
- [15] M. Sangermano, N. Lak, G. Malucelli, A. Samakande, R.D. Sanderson, UV-curing and characterization of polymer-clay nanocoatings by dispersion of acrylate-functionalized organoclays, *Prog. Org. Coat.* 61 (2008) 89–94.
- [16] C.Y. Bai, X.Y. Zhang, J.B. Dai, J.H. Wang, Synthesis of UV crosslinkable waterborne siloxane-polyurethane dispersion PDMS-PEDA-PU and the properties of the films, *J. Coat. Technol. Res.* 5 (2008) 251–257.
- [17] C.Y. Bai, X.Y. Zhang, J.B. Dai, W.H. Li, A new UV curable waterborne polyurethane: effect of C=C content on the film properties, *Prog. Org. Coat.* 55 (2006) 291–295.
- [18] A. Palanisamy, Photo-DSC and dynamic mechanical studies on UV curable compositions containing diacrylate of ricinoleic acid amide derived from castor oil, *Prog. Org. Coat.* 60 (2007) 161–169.
- [19] Q. Yu, S. Nauman, J.P. Santerre, S. Zhu, UV photopolymerization behavior of dimethacrylate oligomers with camphorquinone/amine initiator system, *J. Appl. Polym. Sci.* 82 (2001) 1107–1117.
- [20] K.S. Anseth, C.N. Bowman, N.A. Peppas, Polymerization kinetics and volume relaxation behavior of photopolymerized multifunctional monomers producing highly cross-linked networks, *J. Polym. Sci. Polym. Chem.* 32 (1994) 139–147.
- [21] X.S. Jiang, H.J. Xu, H. Yin, Polymeric amine bearing side-chain thioxanthone as a novel photoinitiator for photopolymerization, *Polymer* 45 (2004) 133–140.
- [22] A. Asif, W.F. Shi, X.F. Shen, K.M. Nie, Physical and thermal properties of UV curable waterborne polyurethane dispersions incorporating hyperbranched aliphatic polyester of varying generation number, *Polymer* 46 (2005) 11066–11078.
- [23] U.W. Gedde, Polymer Physics, Kluwer Academic Publishers, Dordrecht, 1995.
- [24] K. Ueda, H. Kanai, T. Amari, Formability of polyester/melamine pre-painted steel sheets from rheological aspect, *Prog. Org. Coat.* 45 (2002) 267–272.
- [25] D. Santos, H. Raminhos, M.R. Costa, T. Diamantino, F. Goodwin, Performance of finish coated galvanized steel sheets for automotive bodies, *Prog. Org. Coat.* 62 (2008) 265–273.